PHYSICAL REVIEW A **77**, 041608(R) (2008)

Quantum Monte Carlo study of the visibility of one-dimensional Bose-Fermi mixtures

C. N. Varney,[1] V. G. Rousseau,[2] and R. T. Scalettar[1]
[1]*Physics Department, University of California, Davis, California 95616, USA*
[2]*Instituut-Lorentz, Universiteit Leiden, Postbus 9504, 2300 RA Leiden, The Netherlands*
(Received 9 November 2007; published 23 April 2008)

The study of ultracold optically trapped atoms has opened new vistas in the physics of correlated quantum systems. Much attention has now turned to mixtures of bosonic and fermionic atoms. A central puzzle is the disagreement between the experimental observation of a reduced bosonic visibility $\mathcal{V}_b$, and quantum Monte Carlo (QMC) calculations which show $\mathcal{V}_b$ increasing. In this paper, we present QMC simulations which evaluate the density profiles and $\mathcal{V}_b$ of mixtures of bosons and fermions in one-dimensional optical lattices. We resolve the discrepancy between theory and experiment by identifying parameter regimes where $\mathcal{V}_b$ is reduced, and where it is increased. We present a simple qualitative picture of the different response to the fermion admixture in terms of the superfluid and Mott-insulating domains before and after the fermions are included. Finally, we show that $\mathcal{V}_b$ exhibits kinks which are tied to the domain evolution present in the pure case, and also additional structure arising from the formation of boson-fermion molecules, a prediction for future experiments.

DOI: 10.1103/PhysRevA.77.041608 PACS number(s): 03.75.Mn, 03.65.Yz, 03.75.Hh, 71.10.Pm

It has been widely suggested that the strong correlations responsible for magnetism, superconductivity, and the metal-insulator transition in the solid state can be studied via ultracold optically trapped atoms. Indeed, this idea has been successfully realized in the context of both bosonic and fermionic atoms. In the former case, the transition between condensed (superfluid) and insulating phases was demonstrated through the evolution of the interference pattern after the release and expansion of the gas [1]. Initial studies focused on the height [1] and width [2] of the central interference peak, with later work looking at the visibility $\mathcal{V}$, which measures the difference between the maxima and minima of the momentum distribution function $S(\mathbf{k})$ [3–5]. Interesting "kinks" are observed in $\mathcal{V}$ which are associated with the redistribution of the density as the superfluid shells evolve into insulating regions [6,7]. For trapped fermions [8–12], Mott phases could also form [13–15], however, without a signal in $S(\mathbf{k})$. Instead, the evolution of the kinetic energy has been proposed as a means to pinpoint the transition [16].

Attention has turned at present to multicomponent systems, which offer a rich set of phenomena including crossover between Bose-Einstein condensation (BEC) and BCS pairing for two attractive fermionic species and Fulde-Ferrell-Larkin-Ovchinnikov phases in situations with two imbalanced fermion populations. Two recent experimental papers report the effect of the addition of fermionic ^{40}K atoms on the visibility of bosonic ^{87}Rb in a three-dimensional trap [17,18]. The basic result is a decrease in the bosonic visibility $\mathcal{V}_b$ driven by the fermion admixture. A large number of qualitative explanations has been put forth for this phenomenon, including the localization of the bosons by the random fermionic impurities, the segmentation of the bosonic superfluid, the adiabatic heating of the bosonic cloud when the lattice depth is increased in the presence of the two species, an enhanced bosonic mass due to the coupling to the fermions, and the growth of Mott-insulating regions. A fundamental difficulty is that exact quantum Monte Carlo (QMC) calculations show an increase in $\mathcal{V}_b$ [19], in disagreement with experiment. In this paper we resolve this issue.

The behavior of Bose-Fermi mixtures has attracted considerable theoretical attention. The Hamiltonian was derived and its parameters linked to experimental quantities by Albus *et al.* [20]. The equilibrium phase diagram has been studied using mean-field theory and Gutzwiller decoupling [20–22], perturbation theory [21], dynamical mean-field theory (DMFT) [22], exact diagonalization [23], quantum Monte Carlo methods [19,24–26], and density matrix renormalization group (DMRG) [19,27]. The results of these studies include the observation of Mott-insulating phases at "double half-filling," anticorrelated winding of the two species of quantum particles, molecule formation, and precise determination of the exponents characterizing correlation function decay in the different phases. The behavior of the visibility was addressed by Pollet *et al.* [19], who find interesting nonmonotonic structures with fermion density. However, $\mathcal{V}_b$ is always increased relative to the pure case [28].

In this paper we explore the visibility of Bose-Fermi mixtures in one dimension using QMC simulations with the canonical worm algorithm [29–31]. While previous QMC studies have reported a growth of $\mathcal{V}_b$, we show that a significant reduction, such as seen experimentally, is also possible without invoking temperature effects [19]. The enhancement (reduction) of $\mathcal{V}_b$ caused by the disruption (inducement) of the bosonic Mott-insulator phase by the boson-fermion interactions. $\mathcal{V}_b$ also exhibits kinks reminiscent of those in the pure boson case. In the subsequent sections we write down the Hamiltonian and observables and briefly discuss the QMC algorithm. We then present the evolution of $\mathcal{V}_b$ with fermion concentration, its interpretation in terms of the bosonic density profiles, and evidence for the formation of a molecular superfluid in the trap center.

The one-dimensional (1D) Bose-Fermi Hubbard Hamiltonian is [20]

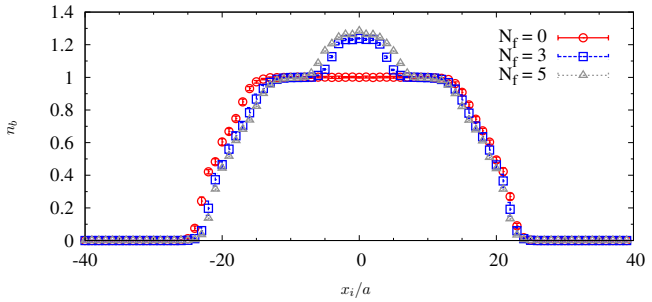

FIG. 1. (Color online) Comparison of the density profiles at $U_{bb}=8.3t$ and $U_{bf}=-5.0t$ for $N_f=0,3,5$ fermions on an 80-site chain with 40 bosons. The Mott insulator at the trap center for the pure bosonic case is destroyed by the addition of fermions. This drives the increase in the visibility.

$$H = -t_b \sum_j (\hat{b}_j^\dagger \hat{b}_{j+1} + \text{H.c.}) - t_f \sum_j (\hat{c}_j^\dagger \hat{c}_{j+1} + \text{H.c.}) + W \sum_i x_i^2 (\hat{n}_b^{(i)} + \hat{n}_f^{(i)}) + \frac{U_{bb}}{2} \sum_i \hat{n}_b^{(i)} (\hat{n}_b^{(i)} - 1) + U_{bf} \sum_i \hat{n}_b^{(i)} \hat{n}_f^{(i)}, \quad (1)$$

where $\hat{b}_j$ ($\hat{b}_j^\dagger$) and $\hat{c}_j$ ($\hat{c}_j^\dagger$) are the annihilation (creation) operators of the bosons and (spin-polarized) fermions at lattice site j, respectively, and $\hat{n}_b^{(i)}=\hat{b}_i^\dagger \hat{b}_i$, $\hat{n}_f^{(i)}=\hat{c}_i^\dagger \hat{c}_i$ are the corresponding number operators. The first two terms of Eq. (1) describe bosonic and fermionic nearest-neighbor hopping. The curvature of the trap is W, and the coordinate of the jth site is given by $x_j=ja$, where a is the lattice constant. U_{bb} and U_{bf} are the on-site boson-boson and boson-fermion interactions. In this work we consider 80-site chains with the nearest-neighbor hopping set to be identical for fermions and bosons ($t_b=t_f=t=1$) and trapping potential $W=0.01t$.

In the canonical worm algorithm [29–31] employed in our calculation, operator expectation values are sampled through the introduction of open-ended world lines that extend over equal imaginary time into a path integral expression for the partition function. The properties we study include the kinetic, potential, and trap energies, the density profiles, and the visibility,

$$\mathcal{V} = \frac{S_{\max} - S_{\min}}{S_{\max} + S_{\min}}, \quad (2)$$

where $S_{\max}$ and $S_{\min}$ are the maximum and minimum values of momentum distribution function,

$$S(k) = \frac{1}{L} \sum_{j,l} e^{ik(x_j - x_l)} \langle \hat{b}_j^\dagger \hat{b}_l \rangle. \quad (3)$$

The enhanced visibilities with fermion concentration reported previously [19] are in contrast with the trend to reduced $\mathcal{V}_b$ measured experimentally [17,18]. In Fig. 1, we see the origin of this effect in a system with 40 bosons: the visibility enhancement at large U_{bb} is caused by the destruction of the Mott phase at the trap center by the fermions. It is natural to conjecture that if $n_b^{(i)}<1$ at the trap center the additional attraction due to the fermions could induce Mott-insulating behavior and reduce $\mathcal{V}$. In Fig. 2(a), we show that this expectation is correct. Here, we fix $U_{bb}=12t$ and increase N_b for both the pure case and for a system with fermion number fixed at $N_f=9$ and boson-fermion interaction at $U_{bf}=-5t$. What we observe is that in a window where the boson central density is approaching $n_b^{(i)}=1$ the bosonic visibility is decreased by the presence of the fermions. The cause is clear: if the bosons are poised just below Mott-insulating behavior, then the fermions can induce it. This is supported by a comparison of the density profiles in Fig. 2(b).

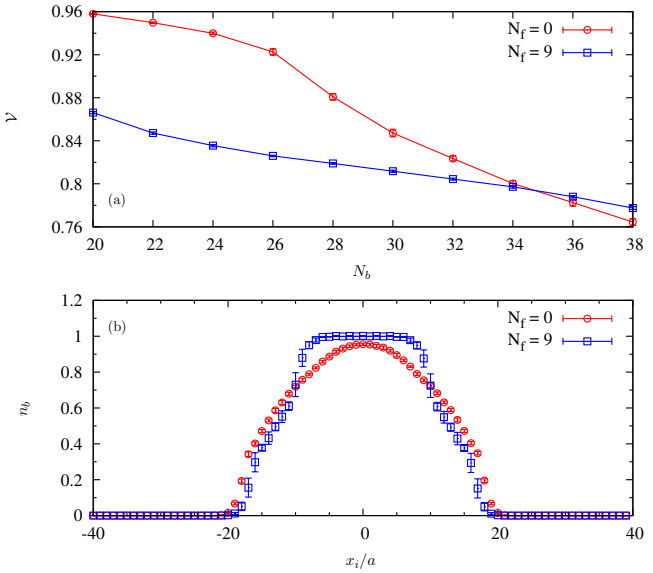

FIG. 2. (Color online) (a) Bosonic visibility $\mathcal{V}_b$ as a function of the number of bosons for $N_f=0$ and 9 fermions with fixed $U_{bb}=12.0t$ and $U_{bf}=-5.0t$. (b) Bosonic density profiles for $N_b=26$ bosons and $N_f=0,9$ fermions. The addition of the fermions induces Mott-insulating behavior in the bosons. The key consequence is a decrease in $\mathcal{V}_b$ for $N_f=9$ relative to $N_f=0$, similar to that seen in the experiments.

The primary mechanism through which fermions affect $\mathcal{V}_b$ is the local adjustment of the site energy and hence of the local bosonic density. This is an effect which occurs regardless of the dimensionality. Hence, we expect aspects of our conclusions to be relevant to experiments in higher dimension [19]. While we have shown a decreased visibility similar to that seen experimentally, the enhancement of visibility may be the more generic behavior in one dimension. In the one-dimensional "state diagram" of the purely bosonic case [32] the area of parameter space occupied by the phase with a Mott plateau of $n_b^{(i)}=2$ is very narrow. Thus the prospect for the fermions to drive the system into this phase is limited.

In the case of a pure bosonic system [7], the change in visibility with the boson-boson interaction strength U_{bb} is not smooth, but is accompanied by "kinks." These kinks are associated with a freezing of the density profile when the transfer of the bosonic density from the trap center is interrupted by the formation of Mott insulator shoulders. In Fig. 3, the behavior of the visibilities and density profiles with U_{bb} in the presence of fermions is shown. $\mathcal{V}_b$ decreases with U_{bb} as

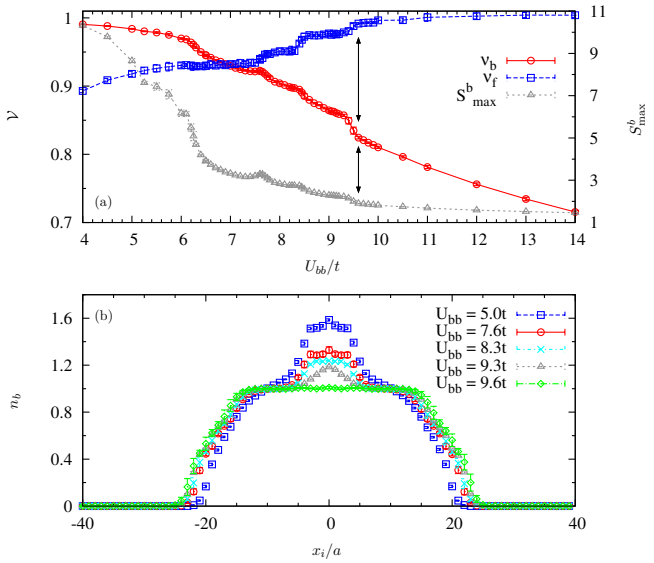

FIG. 3. (Color online) (a) Bosonic and fermionic visibilities and bosonic $S_{\max}$ as functions of U_{bb}/t for a system with 40 bosons, 3 fermions, and $U_{bf}=-5.0t$. The "plateau" regions where the rate of reduction of $\mathcal{V}$ is reduced are due to freezing of the density profiles (see text). The fast decrease after $U_{bb}/t \approx 9.3$ is due to the formation of a Mott-insulating region in the central core, which is fully formed and indicated by the arrow at $U_{bb}/t=9.6$. (b) Boson density profiles at five different values of U_{bb}/t.

the interactions reduce the quasicondensate fraction $S^b_{\max}$. Conversely, the interactions enhance $S^f_{\max}$ and $\mathcal{V}_f$ increases with U_{bb}. There are, however, additional kinks in the case when fermions are present whose origin we shall discuss below. Figure 4 helps to quantify this freezing by showing the evolution of the trap, interaction, and kinetic energies with U_{bb}. These energies exhibit a sequence of plateaus and rapid drops corresponding to the kink locations in Fig. 3.

Figure 5(a) compares the visibility evolution for the pure

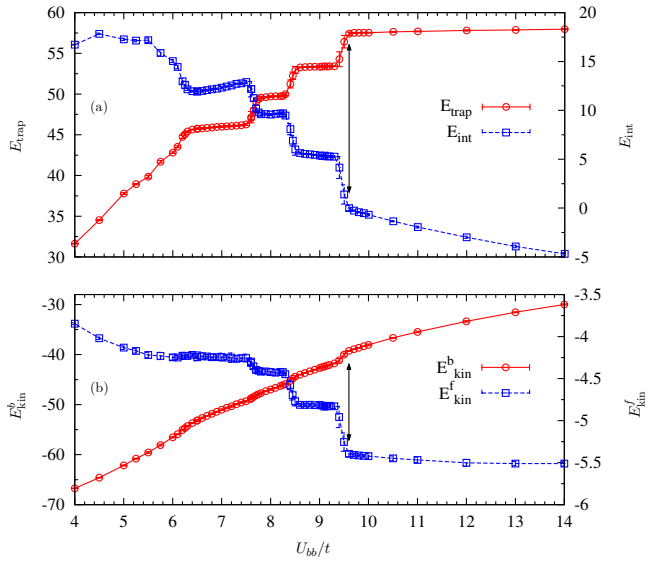

FIG. 4. (Color online) (a) Trapping (E_{trap}) and interaction (E_{int}) energies as functions of U_{bb}/t for the system of Fig. 3 (b) Bosonic (E^b_{kin}) and fermionic (E^f_{kin}) kinetic energies.

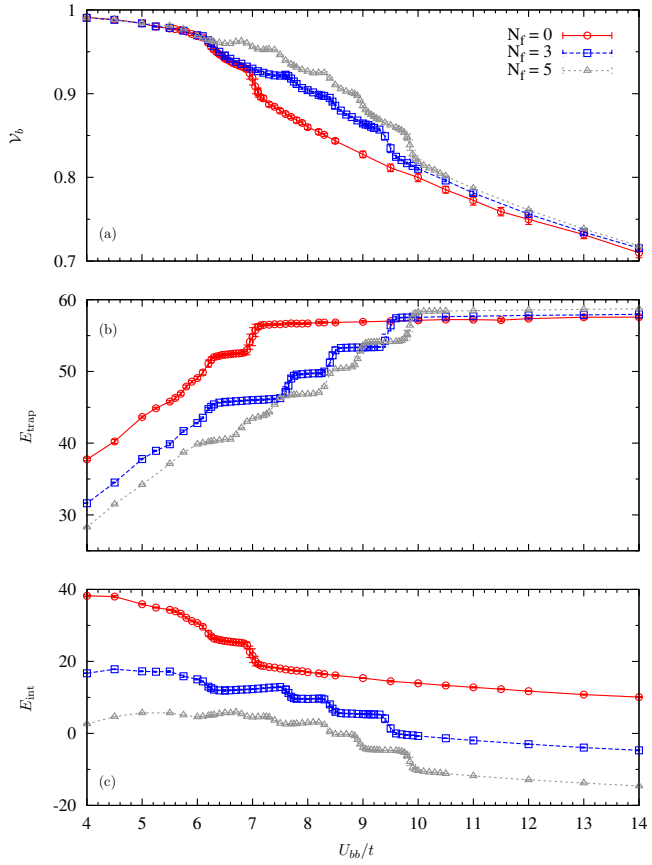

FIG. 5. (Color online) Comparison of (a) bosonic visibility $\mathcal{V}_b$, (b) the trapping energy, and (c) the interaction energy for $N_f=0$, 3, and 5 fermions on an 80-site chain with 40 bosons and fixed $U_{bf}=-5.0t$. The arrows in panels (a), (c), and (b), respectively, denote the locations of the kinks (the onset of rapid change in energy and visibility) for $N_f=0$, 3, and 5 fermions.

bosonic case ($N_f=0$) with two different fermion numbers $N_f=3$ and 5. For $N_f=3$, the kink at lowest $U_{bb}=6.1t$ is associated with the initial emergence of the Mott shoulders. This kink coincides with one in the pure bosonic case $N_f=0$ because the shoulders form outside the regions occupied by the fermions at the trap center. For $N_f=5$, the width of the fermion density is comparable to the size of the bosonic superfluid in the center of the trap, and the kink at $U_{bb}=6.0t$ signifies a freezing of the bosonic density but not the formation of the Mott shoulders. Instead, the kink visible at $U_{bb} \approx 6.8t$ is responsible for the formation of the Mott shoulders. This shift to higher U_{bb} is expected since the attractive U_{bf} delays the transfer of bosonic density out of the center. Figures 5(b) and 5(c) compare the components of the energy. Each plateau signifies that the bosonic and fermionic densities are frozen over the range in U_{bb}. Past experiments [17,18] did not have the resolution to exhibit the kinks we have seen in these simulations; however, they might be seen with improved accuracy.

We also note in Fig. 5 that the number of plateaus is directly related to the number of fermions in the Bose-Fermi mixture and that each plateau is roughly the same size, indicating that bound pairs of bosons and fermions are being destroyed as U_{bb} is increased. This conclusion is substanti-

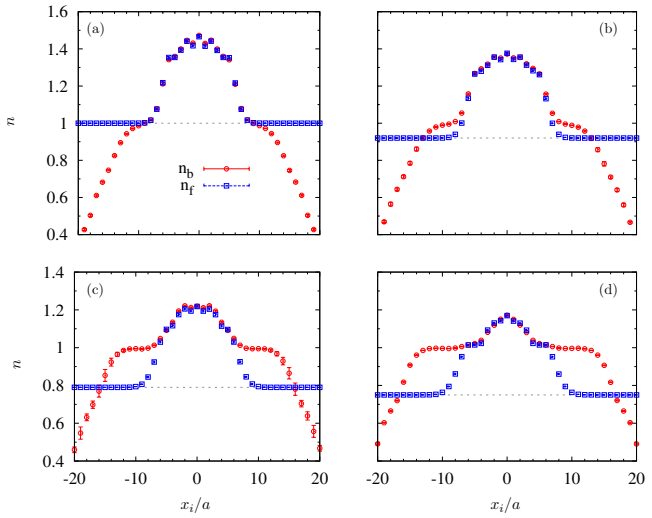

FIG. 6. (Color online) Bosonic and fermionic density profiles for (a) $U_{bb}=6.3t$, (b) $U_{bb}=7.2t$, (c) $U_{bb}=8.6t$, and (d) $U_{bb}=9.5t$ with 5 fermions, 40 bosons, and fixed $U_{bf}=-5.0t$. The fermionic density is offset and the dashed gray line indicates zero density. The densities match in the center of the trap, with the region of coincidence decreasing as U_{bb} increases.

ated in Fig. 6, where we compare the bosonic density with the fermionic density. The fermionic density is offset by a constant to emphasize the near perfect overlap in the densities near the center of the trap, indicating that the trap center is populated by a molecular superfluid (MSF). Indeed, at the weakest coupling, Fig. 6(a), the fermion density precisely equals the excess boson density above the commensurate Mott value $n_b^{(i)}=1$. When U_{bb} is increased, moving from one plateau to another in Fig. 5, the MSF region in the center of the trap shrinks. For the kink at highest U_{bb} ($\approx 9.8t$ for $N_f=5$), the MSF region is destroyed, the bosonic density is a Mott insulator, and the fermionic visibility $\mathcal{V}_f \rightarrow 1$.

In summary, we have shown that the visibility of Bose-Fermi mixtures can be enhanced or reduced by the boson-fermion interactions depending on whether the bosonic density in the pure case is above or below commensuration. This result resolves a fundamental disagreement between experiment and QMC simulations. There are numerous kinks in the visibility and the different energies that result from freezing of the density profiles. While our bosonic component is sufficiently large so that our results are converged with respect to lattice size, the number of fermions is much smaller. It is possible that the kinks will merge together and be less easy to observe in a larger system. The density profiles near the kinks show direct evidence for a molecular superfluid in the center of the trap and that a larger U_{bb} is required to destroy the bound pairs with larger N_f and subsequently induce Mott-insulating behavior.

Supported under the ARO, Contract No. W911NF0710576 under the DARPA OLE program, NSF Contract No. PHY05-51164 (Grant No. NSF-KITP-07-195), and useful input from T. Mavericks.

[1] M. Greiner *et al.*, Nature (London) **415**, 39 (2002).
[2] T. Stöferle, H. Moritz, C. Schori, M. Kohl, and T. Esslinger, Phys. Rev. Lett. **92**, 130403 (2004).
[3] F. Gerbier *et al.*, Phys. Rev. Lett. **95**, 050404 (2005).
[4] F. Gerbier *et al.*, Phys. Rev. A **72**, 053606 (2005).
[5] R. B. Diener, Q. Zhou, H. Zhai, and T. L. Ho, Phys. Rev. Lett. **98**, 180404 (2007).
[6] R. Roth and K. Burnett, Phys. Rev. A **67**, 031602(R) (2003).
[7] P. Sengupta, M. Rigol, G. G. Batrouni, P. J. H. Denteneer, and R. T. Scalettar, Phys. Rev. Lett. **95**, 220402 (2005).
[8] G. Modugno, F. Ferlaino, R. Heidemann, G. Roati, and M. Inguscio, Phys. Rev. A **68**, 011601(R) (2003).
[9] H. Ott *et al.*, Phys. Rev. Lett. **92**, 160601 (2004).
[10] H. Ott *et al.*, Phys. Rev. Lett. **93**, 120407 (2004).
[11] M. Köhl, H. Moritz, T. Stoferle, K. Gunter, and T. Esslinger, Phys. Rev. Lett. **94**, 080403 (2005).
[12] H. Moritz, T. Stoferle, K. Guenter, M. Kohl, and T. Esslinger, Phys. Rev. Lett. **94**, 210401 (2005).
[13] M. Rigol, A. Muramatsu, G. G. Batrouni, and R. T. Scalettar, Phys. Rev. Lett. **91**, 130403 (2003).
[14] M. Rigol and A. Muramatsu, Phys. Rev. A **69**, 053612 (2004).
[15] M. Rigol *et al.*, Opt. Commun. **243**, 33 (2004).
[16] M. Rigol, R. T. Scalettar, P. Sengupta, and G. G. Batrouni, Phys. Rev. B **73**, 121103(R) (2006).
[17] K. Günter, T. Stoferle, H. Moritz, M. Kohl, and T. Esslinger, Phys. Rev. Lett. **96**, 180402 (2006).
[18] S. Ospelkaus *et al.*, Phys. Rev. Lett. **96**, 180403 (2006).
[19] L. Pollet, C. Kollath, U. Schollwock, and M. Troyer, Phys. Rev. A **77**, 023608 (2008).
[20] A. Albus, F. Illuminati, and J. Eisert, Phys. Rev. A **68**, 023606 (2003).
[21] M. Cramer, J. Eisert, and F. Illuminati, Phys. Rev. Lett. **93**, 190405 (2004).
[22] I. Titvinidze, M. Snoek, and W. Hofstetter, Phys. Rev. Lett. **100**, 100401 (2008).
[23] R. Roth and K. Burnett, Phys. Rev. A **69**, 021601(R) (2004).
[24] L. Pollet, M. Troyer, K. Van Houcke, and S. M. A. Rombouts, Phys. Rev. Lett. **96**, 190402 (2006).
[25] P. Sengupta and L. P. Pryadko, Phys. Rev. B **75**, 132507 (2007).
[26] F. Hébert, F. Haudin, L. Pollet, and G. G. Batrouni, Phys. Rev. A **76**, 043619 (2007).
[27] A. Mering and M. Fleischhauer, Phys. Rev. A **77**, 023601 (2008).
[28] For one set of parameters, $\mathcal{V}$ for nonzero N_f falls below the $N_f=0$ value, but only when N_f exceed N_b. In addition, the decrease is less than 10%.
[29] N. V. Prokof'ev *et al.*, JETP **87**, 310 (1998).
[30] S. M. A. Rombouts, K. Van Houcke, and L. Pollet, Phys. Rev. Lett. **96**, 180603 (2006).
[31] K. Van Houcke, S. M. A. Rombouts, and L. Pollet, Phys. Rev. E **73**, 056703 (2006).
[32] G. G. Batrouni *et al.*, Phys. Rev. Lett. **89**, 117203 (2002).